



Enhanced modeling approach for multilayer anisotropic plates based on dimension reduction method and Hellinger–Reissner principle



Ferdinando Auricchio^a, Giuseppe Balduzzi^a, Mohammad Javad Khoshgoftar^{a,b,*}, Gholamhosein Rahimi^{b,*}, Elio Sacco^c

^a Department of Civil Engineering and Architecture, University of Pavia, Pavia, Italy

^b Faculty of Mechanical Engineering, Tarbiat Modares University, Tehran, Iran

^c Department of Civil and Mechanical Engineering, University of Cassino and Southern Lazio, Cassino, Italy

ARTICLE INFO

Article history:

Available online 20 August 2014

Keywords:

Multilayer anisotropic plate modeling
Dimension reduction method
Hellinger–Reissner principle
Plate analytical solution

ABSTRACT

This paper illustrates an innovative approach to obtain an analytical model for elastic, multilayer, anisotropic, and moderately thick plates. The goals of the proposed approach are (i) provide an accurate stress description, (ii) take into account the effects of material anisotropies and inhomogeneities, and (iii) lead to a plate model that does not need shear correction factors.

The first step of the modeling procedure is the weak formulation of the 3D elastic problem. In particular, we choose the Hellinger–Reissner functional expressed in a way that privileges an accurate description of stress field. The second step consists of the reduction of the 3D elastic problem weak formulation to a 2D weak formulation (i.e. the properly called plate-theory) using the dimension reduction method. Finally, the third step allows to obtain the plate-theory strong formulation.

We evaluate some analytical solutions of the obtained plate-theory and we compare them with Classical Plate Theory, First order Shear Deformation Theory, and Elasticity Theory solutions with the aim to evaluate the proposed method accuracy. The results highlight the following main advantages: needless of shear correction factors and accurate description of both stress and displacement fields also in complex situations, like multilayer, anisotropic, and moderately thick plates.

© 2014 Elsevier Ltd. All rights reserved.

1. Introduction

Several laminate theories have been proposed in the literature since the end of 19th century. Among them, Classical Plate Theory (CPT) and First order Shear Deformation Theory (FSDT) are the most famous displacement-based theories, i.e. theories formulated considering only displacements as independent variables.

Based on Kirchhoff–Love assumptions (straight and normal line to the middle-plane before deformation remain straight and normal to the middle-plane also after deformation), CPT neglects shear deformation and could be seen as the generalization of the Euler–Bernoulli beam-theory to 2D problems [1]. CPT accuracy depends on plate span-to-depth ratio, in particular, CPT solution is exact when the span-to-depth ratio goes to infinity [2], but it

becomes more and more inaccurate by decreasing the span-to-depth ratio. Therefore, CPT assumptions are not satisfactory in several practical applications and refined theories are required.

Based on Reissner–Mindlin hypotheses (straight and normal line to the middle-plane before deformation remain straight but not necessarily normal to the middle-plane after deformation), FSDT leads constant shear deformations and shear stresses along thickness to be considered and could be seen as the generalization of the Timoshenko beam-theory to 2D problems [1]. As a consequence, FSDT gives satisfactory results for a larger class of problems compared with CPT [3] but, unfortunately, the span-to-depth ratio continues to influence the model accuracy, the predicted shear stress distribution violates the boundary equilibrium, and shear correction factors must be introduced in order to compute the true amount of shear deformation energy and achieve more accurate results. Real stress distribution and shear correction factor could be easily evaluated for homogeneous plates (in this simple case the shear factor results equal to 5/6). On the other hand, the evaluation of stress distribution and shear correction factor becomes non trivial for multilayer or composite plates. In particular, Whitney [4]

* Corresponding authors. Address: Faculty of Mechanical Engineering, Tarbiat Modares University, Jalal Ale Ahmad Highway, P.O.Box: 14115-111, Tehran, Iran. Tel.: +98 21 82883356; fax: +98 21 82884909.

E-mail addresses: ferdinando.auricchio@unipv.it (F. Auricchio), giuseppe.balduzzi@unipv.it (G. Balduzzi), mj.khoshgoftar@gmail.com (M.J. Khoshgoftar), rahim_gh@modares.ac.ir (G. Rahimi), sacco@unicas.it (E. Sacco).

proposes a simple approach for the estimation of the shear correction factor, whereas, among others, we cite Noor and Burton [5], Auricchio and Sacco [6] as significant approaches for the estimation of the real shear distribution within the thickness. Nevertheless, due to difficulties arising in the estimation process, practitioners often prefer to use 5/6 also for other cases like multilayer in-homogeneous plates, even if it clearly represents an error [1,7]. Moreover, all the so far proposed approaches imply pre-processing and post-processing calculations that are clearly unwanted. As a consequence, researchers develop several theories to overcome the FSDT's limitations so far described and predict effectively the behavior of thick and laminated plates. For a complete review of existing models readers may refer to [8].

Khandan et al. [9] review several laminated composite plate theories and discuss advantages and limitations of each theory, focusing on how accurately and efficiently models can predict the transverse shear effect. They show that enhanced theories must be used in order to effectively describe the behavior of plates with nontrivial properties, specially for laminated plates. As discussed in [8], there exist different paths to improve standard theories and we can classify enhanced theories in many categories: looking at considered approximations we can distinguish between the higher order shear deformation and the layer-wise theories, whereas looking at considered independent-variables we can distinguish between the displacement-based and the mixed theories.

The higher order theories are obtained assuming non-linear displacement distribution through the thickness. Lo et al. [10,11] are a classical example of higher order theory whereas as a more recent example we can cite Reddy and Kim [12] that propose a general third order theory for a functionally graded plate with micro structure that depend on length scale parameter. In particular, by choosing third order polynomial for in-plane displacement, the authors obtain third order shear deformation theory and recover FSDT and CPT as special cases of their general model. However, some of the higher order models do not satisfy the continuity conditions of transverse shear stresses at layer interfaces and lead to inaccurate stress description. On the other hand, the layer-wise theories are obtained assuming displacement distribution through each layer and imposing suitable continuities at interfaces [13]. Obviously these models could be extremely accurate, but also expensive [14].

Displacement-based theories consider as independent variables only displacements, as usual for CPT, FSDT standard formulation, and higher-order theories, whereas mixed theories consider also stresses and strains as independent variables. As an example, mixed theories can originate from mixed variational principles like Hellinger–Reissner (HR) and Hu–Whashizu (HW) functionals. More in detail, HR functional considers displacement and stress as independent variables whereas HW functional considers also strain [15]. Unfortunately, as stated by Brezzi [16], mixed variational principles and the related theories are more delicate than the displacement-based theories since mixed functionals may work well for specific problems but work poorly in general conditions. Moreover, to ensure and prove stability and convergence of a mixed theory is a non-trivial achievement [17]. Nevertheless, mixed principles are widely used in plate and shell theory development as well as in development of discretization techniques like Finite Elements since their advantages exceed their limitations and costs. As significant examples of mixed theories we mention Bisegna and Sacco [18], Auricchio and Sacco [19] that use the so far introduced mixed variational formulation together with the FSDT displacement assumptions in order to improve the FSDT stress description. In the following, we focus our attention on layer-wise, mixed variational theories since they provide an accurate stress description, in agreement with the job's aims.

For completeness in discussion of mixed variational principles, we cite also the so called Reissner Mixed Variational Theorem (RMVT) that uses only shear stresses as independent variables [20–22] and that was extensively used in both plate model and Finite-Element derivation [23,24]. Carrera [25] presents the comparison of classical theories formulated on basis of principle of virtual displacement and mixed theories based on the RMVT, considering both global and local responses of multilayer orthotropic plates. He concluded that the RMVT based theories are superior with respect to the Principle of Virtual Displacements based theories. Also Carrera and Demasi [26] derive a plate-theory based on RMVT and, more recently, Demasi [27–31] develop a generalized unified formulation with the aims to investigate the RMVT based theories and compare a variety of mixed first- and high- order shear deformation theories as well as global, zig-zag, and layer-wise theories. Wu and Li [32,33] investigate the static behavior of simply supported multilayer composite and functionally graded material plate. In particular, they consider both RMVT and the principle of virtual displacement in order to develop a RMVT-based Shear Deformation Theory.

Balduzzi [34] presents the HR and HW functionals and discusses their primal and dual formulation, highlighting that the primal formulation privileges the regularity of displacement approximation whereas the dual formulation privileges the regularity of stress approximation. He reviews also the applications in beam and plate modeling of both formulations, noticing that the dual formulation is not so diffused in engineering practice, maybe as a consequence of difficulties occurring in discretization of the involved functional spaces. Nevertheless, the promising results illustrated by Balduzzi [34] lead us to focus our attention on the HR dual formulation since it provides equations more significant than the primal. Also Alessandrini et al. [35] derive a plate-theory for an homogeneous, isotropic, and linearly elastic body using both primal- and dual- HR functional formulations. Specifically, Alessandrini et al. [35] use the dimension reduction method, prove the existence and uniqueness of the solution of the partial differential equations corresponding to the plate-theory, and provide modeling error bounds for both formulations. Also Liu [36] uses the dimension reduction method for elasticity plate on an unbounded domain, estimates error between the exact- and the reduced- solutions, and shows the method capabilities in the field of plate modeling. The so far mentioned dimension reduction method is a mathematical procedure that introduces some approximations in a variational principle with the aim to solve a $(n + 1)$ dimension boundary value problem by replacing it with a system of equations in n dimension space. More in details, the procedure is firstly proposed by Kantorovich and Krylov [37] whereas, among others, Vogelius and Babuska [38] use the dimension reduction method to drive a displacement based plate-theory with linear displacement distribution.

In addition to all the so far introduced theories, we must mention that Pagano [39] publishes the analytical solution of the 3D elastic problem for a rectangular laminated plate with pined edged and made of orthotropic materials with material symmetry axes parallel to plate axes. The plate elasticity solution can be evaluated only assuming simple geometry, loads, and boundary conditions. Moreover, it requires heavy computational process since the number of variables depends on the number of layers. As a consequence, the elasticity solution is impractical for engineering applications, nevertheless it remains a fundamental reference for the evaluation of the plate-theory capabilities. In addition, Pagano [39] compares elasticity solution with classical laminated plate-theory and shows that the accuracy of classical plate theories depends on material properties, geometry, and span-to-depth ratio. Finally the author notices that the 3D-elasticity and CPT solutions could be extremely far for multilayer plates.

Despite the focus of the present paper limits to plate-theory derivation, we find useful to mention that mixed variational principles could be used also for plate finite element derivation. For instance, by adopting a mixed enhanced variational formulation and first order shear deformation theory, Auricchio and Sacco [40] present a finite element method for the analysis of laminated composite plates with an accurate evaluation of shear correction factor. More recently, Daghia et al. [41] present another mixed theory based on FSDT and the corresponding quadratic, four-node finite element based on mixed stress formulation. Finally, Moleiro et al. [42] propose a layer-wise finite element model developed in a mixed least square formulation for static analysis of multilayer composite plates, obtaining numerical solutions in agreement with 3D solution.

Auricchio et al. [43] introduce a new modeling approach for planar linear elastic beams based on HR principle. Specifically, they specialize the approach suggested by Alessandrini et al. [35] to 2D problems and develop a planar beam multilayer models based on dimension reduction approach and HR principle. The obtained model is extremely accurate and has the capability to capture the local effects produced by boundary constrains and load distribution. Moreover, shear correction factor appears naturally from the variational derivation. More recently Auricchio et al. [44] generalize the planar beam-theory to the case of 3D beams.

In the present paper, we generalize the modeling approach presented by Auricchio et al. [43] to multilayer, anisotropic plates. In Section 2, thickness shape functions with arbitrary coefficients are adopted for both displacement and stress field and, then, plate-theory partial differential equations are derived starting from the HR dual formulation. In Section 3, we discuss how to obtain the analytical solutions for CPT, FSDT, elasticity solution, and the plate-theory introduced in this paper. Finally, in Section 4, the most important plate-theories are compared with the Current Work in order to highlight capabilities and limitations of the proposed modeling approach.

The main goals of the current work is to obtain a plate-theory that:

1. provides an accurate description of both stress and displacement fields also in complex situations like multilayer, anisotropic, and moderately thick plates; in particular, we devote special emphasis to an accurate stress description since it govern fundamental phenomena like failure
2. does not need any correction factor that must be evaluated a priori
3. does not need any a posteriori processing, e.g. in order to recover the stress thickness-distribution
4. could be generalized to complex situations, e.g. graded plates or non-linear constitutive laws
5. could use arbitrarily-accurate variable-descriptions, in order to adapt to specific practitioners needs

2. Theory derivation

In this chapter we derive an enhanced plate mixed theory. In SubSection 2.1 we perform the first step of the modeling procedure, i.e. the weak formulation of the 3D elastic problem, in SubSection 2.2 we perform the second step, i.e. the reduction of the 3D problem to a 2D problem through the dimension reduction method, in SubSection 2.3 we perform the third step that consists of few analytical calculations that allow the partial differential equations governing the plate-theory to be obtained. Finally, in SubSection 2.4 we show that the proposed modeling approach, together with suitable assumptions, allows the FSDT partial differential equations to be recovered, with also the capability to

take into account the right amount of shear deformation energy (i.e. without the need of any further shear correction factor).

2.1. Problem definition

We introduce the plate middle-plane A that is a closed and bounded set of \mathbb{R}^2 defined as follows:

$$A = \{(x, y) \in \mathbb{R}^2 | A \text{ closed and bounded}\} \quad (1)$$

Moreover, we assume that its boundary, denoted as ∂A is a sufficiently smooth line. In addition, we introduce the plate thickness h that is defined as follows:

$$h = \left\{ z \in \mathbb{R} | z \in \left[-\frac{\bar{h}}{2}, \frac{\bar{h}}{2} \right] \right\} \quad (2)$$

where \bar{h} denotes the measure of the plate thickness. In consequence of the so far introduced sets, the problem domain Ω is defined as follows:

$$\Omega = A \times h \quad (3)$$

Fig. 1 represents the problem domain Ω , the adopted Cartesian coordinate system, plate middle-plane A , and the middle-plane boundary ∂A .

We denote the domain boundary as $\partial\Omega$ and we consider the partition $\{\partial\Omega_s; \partial\Omega_t\}$. $\partial\Omega_s$ denotes the displacement constrained boundary and in the following we assume that $\partial\Omega_s = \partial A \times h$. On the other hand, $\partial\Omega_t$ denotes the loaded boundary that, as a consequence results as $\partial\Omega_t = A \times \left(-\frac{\bar{h}}{2}, \frac{\bar{h}}{2}\right)$ (see Fig. 2).

The mixed problem variables are the displacement vector field $\mathbf{s} : \Omega \rightarrow \mathbb{R}^3$, the symmetric stress tensor field $\boldsymbol{\sigma} : \Omega \rightarrow \mathbb{R}_s^{3 \times 3}$, and the corresponding virtual fields $\delta\mathbf{s}$ and $\delta\boldsymbol{\sigma}$.

The boundary conditions are defined as:

$$\mathbf{s} = \bar{\mathbf{s}} \text{ on } \partial\Omega_s; \quad \boldsymbol{\sigma} \cdot \mathbf{n} = \mathbf{t} \text{ on } \partial\Omega_t \quad (4)$$

where $\bar{\mathbf{s}} : \partial\Omega_s \rightarrow \mathbb{R}^3$ is the assigned boundary displacement that is assumed to be a sufficiently smooth function, $\mathbf{t} : \partial\Omega_t \rightarrow \mathbb{R}^3$ is the assigned boundary load distribution, and \mathbf{n} is the outward unit vector, defined on the boundary surface. We highlight that the boundary-conditions (4) ensure that the 3D problem is well-posed but lead only the clamp to be considered as admissible displacement constraint. Obviously, this assumption could appear too restrictive for an enhanced plate-theory, nevertheless the derivation procedure leads the boundary conditions to be managed in a way that recovers also other displacement constraints as the simply support without further complications (see Section 2.3). Finally, for notation simplicity, we are going to neglect the boundary load (i.e. we assume $\mathbf{t} = \mathbf{0}$), nevertheless this hypothesis is not necessary in plate-theory derivation and it could be easily removed.

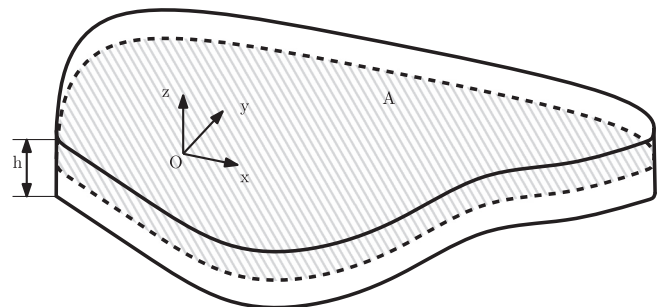


Fig. 1. Problem domain, adopted Cartesian coordinate system, notations, and dimensions.

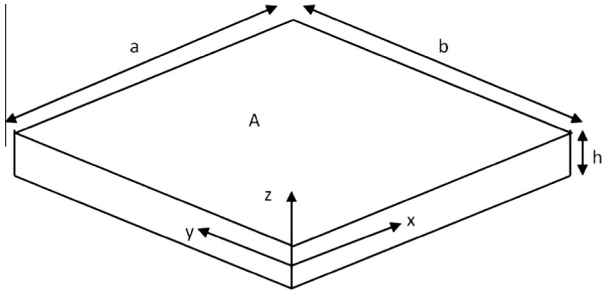


Fig. 2. Rectangular plate: coordinate system and dimensions.

Last but not least, we introduce the volume force density $\mathbf{f} : \Omega \rightarrow \mathbb{R}^3$ and the fourth-order elastic tensor \mathbf{D} that describes the linear constitutive law of the anisotropic material constituting the plate.

Introducing the following spaces:

$$\begin{aligned} L^2(\Omega) &= \left\{ \mathbf{s} : \Omega \rightarrow \mathbb{R}^3 : \int_{\Omega} \mathbf{s} \cdot \mathbf{s} \, d\Omega < \infty \right\} \\ H(\text{div}, \Omega) &= \{ \boldsymbol{\sigma} : \Omega \rightarrow \mathbb{R}^{3 \times 3} : \boldsymbol{\sigma} \text{ and } \text{div}(\boldsymbol{\sigma}) \in L^2(\Omega) \} \\ W &= \{ \mathbf{s} \in L^2(\Omega) \}; \quad S := \{ \delta \boldsymbol{\sigma} \in H(\text{div}, \Omega) : \delta \boldsymbol{\sigma} \cdot \mathbf{n}|_{\partial\Omega_t} = \mathbf{0} \} \end{aligned} \quad (5)$$

the 3D elastic problem could be formulated through the following variational equation.

Find $\mathbf{s} \in W$ and $\boldsymbol{\sigma} \in S$ such that $\forall \delta \mathbf{s} \in W$ and $\forall \delta \boldsymbol{\sigma} \in S$

$$\begin{aligned} \delta J_{HR} := & \int_{\Omega} \delta \mathbf{s} \cdot \text{div}(\boldsymbol{\sigma}) \, d\Omega + \int_{\Omega} \text{div}(\delta \boldsymbol{\sigma}) \cdot \mathbf{s} \, d\Omega + \int_{\Omega} \delta \boldsymbol{\sigma} : \mathbf{D} : \boldsymbol{\sigma} \, d\Omega \\ & + \int_{\Omega} \delta \mathbf{s} \cdot \mathbf{f} \, d\Omega - \int_{\partial\Omega_s} \delta \boldsymbol{\sigma} \cdot \mathbf{n} \cdot \bar{\mathbf{s}} \, dA = 0 \end{aligned} \quad (6)$$

that corresponds to the dual formulation of the HR functional. As anticipated in Section 1, we highlight that Eq. (6) uses stress field more regular than displacement field.

2.2. Dimension reduction

Following the notation introduced by Alessandrini et al. [35], we represent the displacement \mathbf{s} and the stress tensor $\boldsymbol{\sigma}$ as illustrated in the following:

$$\mathbf{s} = \begin{Bmatrix} u \\ v \\ w \end{Bmatrix} = \begin{Bmatrix} \mathbf{u} \\ \mathbf{w} \end{Bmatrix}; \quad \boldsymbol{\sigma} = \begin{Bmatrix} \sigma_x & \tau_{xy} & \tau_{xz} \\ \tau_{xy} & \sigma_y & \tau_{yz} \\ \tau_{xz} & \tau_{yz} & \sigma_z \end{Bmatrix} = \begin{Bmatrix} \boldsymbol{\zeta} & \boldsymbol{\tau} \\ \boldsymbol{\tau}^T & \zeta \end{Bmatrix} \quad (7)$$

where

- $\mathbf{u} : \Omega \rightarrow \mathbb{R}^2$ represents the in-plane displacements
- $w : \Omega \rightarrow \mathbb{R}$ represents the out-of-plane displacement
- $\boldsymbol{\zeta} : \Omega \rightarrow \mathbb{R}^{2 \times 2}$ represents the in-plane stresses
- $\boldsymbol{\tau} : \Omega \rightarrow \mathbb{R}^2$ represents the out-of-plane shear-stresses
- $\zeta : \Omega \rightarrow \mathbb{R}$ represents the out-of-plane stress

We highlight that the so far introduced notation has the following analogies and differences with the “classical” plate-theory variables:

- \mathbf{u} contains informations about the membrane displacements and bending rotations
- w contains informations about the out-of-plane displacement
- $\boldsymbol{\zeta}$ contains informations about the membrane stresses and the bending moments
- $\boldsymbol{\tau}$ contains informations about the out-of-plane shear stresses
- ζ is usually neglected in classical plate modeling

Consistently with Definitions (7), we introduce also the following notations:

$$\text{div}(\cdot) = \left\{ \begin{array}{l} \frac{\partial}{\partial x} \\ \frac{\partial}{\partial y} \\ \frac{\partial}{\partial z} \end{array} \right\} = \left\{ \begin{array}{l} \text{div}_A(\cdot) \\ \frac{\partial}{\partial z} \end{array} \right\}; \quad \mathbf{f} = \begin{Bmatrix} f_x \\ f_y \\ f_z \end{Bmatrix} = \begin{Bmatrix} \mathbf{f}_A \\ f_z \end{Bmatrix}; \quad \bar{\mathbf{s}} = \begin{Bmatrix} \bar{u} \\ \bar{v} \\ \bar{w} \end{Bmatrix} = \begin{Bmatrix} \bar{\mathbf{u}} \\ \bar{w} \end{Bmatrix} \quad (8)$$

Introducing Definitions (7) and the notations introduced in Eqs. (8) and (6) can be re-wrote as follows:

$$\begin{aligned} \delta J_{HR} := & \int_{\Omega} \left(\delta \mathbf{u} \cdot \text{div}_A(\boldsymbol{\zeta}) + \delta \mathbf{u} \cdot \frac{\partial}{\partial z} \boldsymbol{\tau} + \delta w \text{div}_A(\boldsymbol{\tau}) + \delta w \frac{\partial}{\partial z} \zeta \right) d\Omega \\ & + \int_{\Omega} \left(\text{div}_A(\delta \boldsymbol{\zeta}) \cdot \mathbf{u} + \frac{\partial}{\partial z} \delta \boldsymbol{\tau} \cdot \mathbf{u} + \text{div}_A(\delta \boldsymbol{\tau}) w + \frac{\partial}{\partial z} \delta \zeta w \right) d\Omega \\ & + \int_{\Omega} (\delta \boldsymbol{\zeta} : \mathbf{D}_{AA} : \boldsymbol{\zeta} + \delta \boldsymbol{\zeta} : \mathbf{D}_{At} \cdot \boldsymbol{\tau} + \delta \boldsymbol{\zeta} : \mathbf{D}_{Ah} \boldsymbol{\zeta} + \delta \boldsymbol{\tau} \cdot \mathbf{D}_{tA} : \boldsymbol{\zeta} \\ & + \delta \boldsymbol{\tau} \cdot \mathbf{D}_{\tau\tau} \cdot \boldsymbol{\tau} + \delta \boldsymbol{\tau} \cdot \mathbf{D}_{th} \boldsymbol{\zeta} + \delta \zeta \mathbf{D}_{hA} : \boldsymbol{\zeta} + \delta \zeta \mathbf{D}_{ht} \cdot \boldsymbol{\tau} + \delta \zeta \mathbf{D}_{hh} \zeta) \, d\Omega \\ & + \int_{\Omega} (\delta \mathbf{u} \cdot \mathbf{f}_A + \delta w f_z) \, d\Omega - \int_{\partial\Omega_s} (\delta \boldsymbol{\zeta} \cdot \mathbf{n}_A \cdot \bar{\mathbf{u}} + \delta \boldsymbol{\tau} \cdot \mathbf{n}_A \bar{w}) \, dA = 0 \end{aligned} \quad (9)$$

where

- $\mathbf{D}_{AA} : h \rightarrow \mathbb{R}^{2 \times 2 \times 2 \times 2}$ is a fourth order tensor
- $\mathbf{D}_{At} = \mathbf{D}_{tA}^T : h \rightarrow \mathbb{R}^{2 \times 2 \times 2}$ is a third order tensor
- $\mathbf{D}_{Ah} = \mathbf{D}_{hA}^T : h \rightarrow \mathbb{R}^{2 \times 2}$ is a second order tensor
- $\mathbf{D}_{\tau\tau} : h \rightarrow \mathbb{R}^{2 \times 2}$ is a second order tensor
- $\mathbf{D}_{th} = \mathbf{D}_{ht}^T : h \rightarrow \mathbb{R}^2$ is a first order tensor
- $D_{hh} : h \rightarrow \mathbb{R}$ is a scalar

All them represent a suitable decomposition of the fourth-order linear elastic tensor \mathbf{D} . Moreover we notice that $\mathbf{n}|_{\partial\Omega_s} = \{\mathbf{n}_A^T, 0\}^T$.

The dimension reduction continues with the introduction of the approximation of each unknown field $\boldsymbol{\gamma} : \Omega \rightarrow \mathbb{R}^{(l)}$ that is expressed as the linear combination of n_γ assigned and linearly independent thickness shape functions $\hat{\boldsymbol{\gamma}} : h \rightarrow \mathbb{R}$, defined together with an element of the image space $\bar{\boldsymbol{\gamma}} \in \mathbb{R}^{(l)}$, and weighted with arbitrary coefficient functions $\tilde{\boldsymbol{\gamma}} : A \rightarrow \mathbb{R}$. As a consequence it results that:

$$\boldsymbol{\gamma}(x, y, z) = \sum_{i=1}^{n_\gamma} \hat{\boldsymbol{\gamma}}_i(z) \bar{\boldsymbol{\gamma}}_i \tilde{\boldsymbol{\gamma}}_i(x, y) \quad (10)$$

In other words, the notation introduced in Eq. (10) allows the thickness approximation $\hat{\boldsymbol{\gamma}}_i(z)$ to be distinguished, the image space structure $\bar{\boldsymbol{\gamma}}$, and the scalar functions $\tilde{\boldsymbol{\gamma}}_i(x, y)$ that will become the unknowns of the partial differential equations governing the plate-theory.

In order to explain better the so far introduced notation, we introduce a simple example. If we assume that the in-plane displacements are linear with respect to the thickness coordinate as illustrated in the following, we need 4 independent degrees of freedom in order to describe the in-plane kinematic.

$$\mathbf{u}(x, y, z) = \begin{Bmatrix} u_0(x, y) + z \varphi_x(x, y) \\ v_0(x, y) + z \varphi_y(x, y) \end{Bmatrix} \quad (11)$$

Using the notation introduced in Eq. (10), we fix $n_u = 4$ and the linear combination terms result defined as follows:

$$\begin{aligned} \hat{u}_1(z) &= 1; & \bar{\mathbf{u}}_1 &= \{1, 0\}^T; & \tilde{u}_1(x, y) &= u_0(x, y) \\ \hat{u}_2(z) &= z; & \bar{\mathbf{u}}_2 &= \{0, 1\}^T; & \tilde{u}_2(x, y) &= v_0(x, y) \\ \hat{u}_3(z) &= z; & \bar{\mathbf{u}}_3 &= \{1, 0\}^T; & \tilde{u}_3(x, y) &= \varphi_x(x, y) \\ \hat{u}_4(z) &= z; & \bar{\mathbf{u}}_4 &= \{0, 1\}^T; & \tilde{u}_4(x, y) &= \varphi_y(x, y) \end{aligned} \quad (12)$$

In Eq. (10) we write explicitly the dependencies of the variables on the Cartesian coordinates, nevertheless in the following we are going to omit this information for notation simplicity.

As a consequence of assumption (10), the approximations of variables introduced in Eq. (8) can be expressed as:

$$\begin{aligned} \mathbf{u} &= \sum_{i=1}^{n_u} \hat{u}_i \bar{\mathbf{u}}_i \tilde{u}_i & \delta \mathbf{u} &= \sum_{j=1}^{n_u} \hat{u}_j \bar{\mathbf{u}}_j \delta \tilde{u}_j & \mathbf{w} &= \sum_{k=1}^{n_w} \hat{w}_k \bar{\mathbf{w}}_k & \delta \mathbf{w} &= \sum_{l=1}^{n_w} \hat{w}_l \delta \tilde{w}_l \\ \boldsymbol{\zeta} &= \sum_{p=1}^{n_\zeta} \hat{\zeta}_p \bar{\boldsymbol{\zeta}}_p \tilde{\zeta}_p & \delta \boldsymbol{\zeta} &= \sum_{q=1}^{n_\zeta} \hat{\zeta}_q \bar{\boldsymbol{\zeta}}_q \delta \tilde{\zeta}_q & \boldsymbol{\tau} &= \sum_{r=1}^{n_\tau} \hat{\tau}_r \bar{\boldsymbol{\tau}}_r \tilde{\tau}_r & \delta \boldsymbol{\tau} &= \sum_{s=1}^{n_\tau} \hat{\tau}_s \bar{\boldsymbol{\tau}}_s \delta \tilde{\tau}_s \\ \boldsymbol{\zeta} &= \sum_{t=1}^{n_\zeta} \hat{\zeta}_t \tilde{\boldsymbol{\zeta}}_t & \delta \boldsymbol{\zeta} &= \sum_{v=1}^{n_\zeta} \hat{\zeta}_v \delta \tilde{\boldsymbol{\zeta}}_v \end{aligned} \quad (13)$$

In particular, we remark that:

- despite the different indexes, the same thickness shape functions describe both the variables and the corresponding variations, e.g. if $i = j \Rightarrow \hat{u}_i = \hat{u}_j$ and $\bar{\mathbf{u}}_i = \bar{\mathbf{u}}_j$

$$\begin{aligned} G_{jp} &= G_{qi} = \int_h \hat{u}_j \hat{a}_p dz \text{ for } i = j \text{ and } q = p & G_{jr} &= G_{si} = \int_h \hat{u}_j \hat{\tau}'_r dz \text{ for } i = j \text{ and } s = r \\ G_{lr} &= G_{sk} = \int_h \hat{w}_l \hat{\tau}_r dz \text{ for } k = l \text{ and } s = r & G_{lt} &= G_{vk} = \int_h \hat{w}_l \hat{\zeta}'_t dz \text{ for } k = l \text{ and } v = t \\ G_{qp} &= \int_h \hat{a}_q \hat{a}_p dz & G_{qr} &= G_{sp} = \int_h \hat{a}_q \hat{\tau}_r dz \text{ for } p = q \text{ and } s = r \\ G_{qt} &= G_{vp} = \int_h \hat{a}_q \hat{\zeta}'_t dz \text{ for } p = q \text{ and } v = t & G_{sr} &= \int_h \hat{\tau}_s \hat{\tau}_r dz \\ G_{st} &= G_{vr} = \int_h \hat{\tau}_s \hat{\zeta}'_t dz \text{ for } v = t \text{ and } r = s & G_{vt} &= \int_h \hat{\zeta}_v \hat{\zeta}'_t dz \\ \mathbf{F}_j &= \int_h \hat{u}_j \mathbf{f}_A dz & \mathbf{F}_l &= \int_h \hat{w}_l \mathbf{f}_z dz \\ \bar{\mathbf{U}}_q &= \int_h \hat{a}_q \bar{\mathbf{u}} dz & \bar{\mathbf{W}}_s &= \int_h \hat{\tau}_s \bar{\mathbf{w}} dz \end{aligned} \quad (16)$$

- since w , δw , ζ , and $\delta \zeta$ are scalar fields, \bar{w}_k , \bar{w}_l , $\bar{\zeta}_t$, and $\bar{\zeta}_v$ result equal to scalar values and, as a consequence, we neglect them in Eq. (13) and in the following
- the satisfaction of boundary equilibrium (see space definitions (5)) requires that $\forall r \quad \hat{\tau}_r|_{\pm \frac{h}{2}} = 0$ and $\forall t \quad \hat{\zeta}_t|_{\pm \frac{h}{2}} = 0$
- in the following, we are going to use the Einstein notation, in order to simplify expressions.

Substituting Eq. (13) in Eq. (9), the mixed variational equation can be rewritten as:

$$\begin{aligned} \delta J_{HR} &:= \int_{\Omega} (\hat{u}_j \hat{\zeta}_p \delta \tilde{u}_j \bar{\mathbf{u}}_j \cdot \text{div}_A(\bar{\boldsymbol{\zeta}}_p \tilde{\zeta}_p) + \hat{u}_j \hat{\tau}'_r \delta \tilde{u}_j \bar{\mathbf{u}}_j \cdot \bar{\boldsymbol{\tau}}_r \tilde{\tau}_r + \hat{w}_l \hat{\tau}_r \delta \tilde{w}_l \text{div}_A(\bar{\boldsymbol{\tau}}_r \tilde{\tau}_r) \\ &+ \hat{w}_l \hat{\zeta}'_t \delta \tilde{w}_l \tilde{\boldsymbol{\zeta}}_t) d\Omega + \int_{\Omega} (\hat{\zeta}_q \hat{u}_i \text{div}_A(\delta \tilde{\zeta}_q \bar{\boldsymbol{\zeta}}_q) \cdot \bar{\mathbf{u}}_i \tilde{u}_i + \hat{\tau}'_s \hat{u}_i \delta \tilde{\tau}_s \bar{\boldsymbol{\tau}}_s \cdot \bar{\mathbf{u}}_i \tilde{u}_i \\ &+ \hat{\tau}_s \hat{w}_k \text{div}_A(\delta \tilde{\tau}_s \bar{\boldsymbol{\tau}}_s) \bar{\mathbf{w}}_k + \hat{\zeta}'_v \hat{w}_k \delta \tilde{\zeta}_v \bar{\mathbf{w}}_k) d\Omega + \int_{\Omega} (\hat{\zeta}_q \hat{\zeta}_p \delta \tilde{\zeta}_q \bar{\boldsymbol{\zeta}}_q : \mathbf{D}_{AA} : \bar{\boldsymbol{\zeta}}_p \tilde{\zeta}_p \\ &+ \hat{\zeta}_q \hat{\tau}_r \delta \tilde{\zeta}_q \bar{\boldsymbol{\zeta}}_q : \mathbf{D}_{A\tau} \cdot \bar{\boldsymbol{\tau}}_r \tilde{\tau}_r + \hat{\zeta}_q \hat{\zeta}_t \delta \tilde{\zeta}_q \bar{\boldsymbol{\zeta}}_q : \mathbf{D}_{A\zeta} \tilde{\boldsymbol{\zeta}}_t + \hat{\tau}_s \hat{\zeta}_p \delta \tilde{\tau}_s \bar{\boldsymbol{\tau}}_s \cdot \mathbf{D}_{\tau A} : \bar{\boldsymbol{\zeta}}_p \tilde{\zeta}_p \\ &+ \hat{\tau}_s \hat{\tau}_r \delta \tilde{\tau}_s \bar{\boldsymbol{\tau}}_s \cdot \mathbf{D}_{\tau\tau} \cdot \bar{\boldsymbol{\tau}}_r \tilde{\tau}_r + \hat{\tau}_s \hat{\zeta}_t \delta \tilde{\tau}_s \bar{\boldsymbol{\tau}}_s \cdot \mathbf{D}_{t\zeta} \tilde{\boldsymbol{\zeta}}_t + \hat{\zeta}_v \hat{\zeta}_p \delta \tilde{\zeta}_v \mathbf{D}_{hA} : \bar{\boldsymbol{\zeta}}_p \tilde{\zeta}_p \\ &+ \hat{\zeta}_v \hat{\tau}_r \delta \tilde{\zeta}_v \mathbf{D}_{h\tau} \cdot \bar{\boldsymbol{\tau}}_r \tilde{\tau}_r + \hat{\zeta}_v \hat{\zeta}_t \delta \tilde{\zeta}_v \mathbf{D}_{hh} \tilde{\boldsymbol{\zeta}}_t) d\Omega + \int_{\Omega} (\hat{u}_j \delta \tilde{u}_j \bar{\mathbf{u}}_j \cdot \mathbf{f}_A + \hat{w}_l \delta \tilde{w}_l \bar{\mathbf{f}}_z) d\Omega \\ &- \int_{\partial \Omega_s} (\hat{\zeta}_q \delta \tilde{\zeta}_q \bar{\boldsymbol{\zeta}}_q \cdot \mathbf{n}_A \cdot \bar{\mathbf{u}} + \hat{\tau}_s \delta \tilde{\tau}_s \bar{\boldsymbol{\tau}}_s \cdot \mathbf{n}_A \bar{\mathbf{w}}) dA = 0 \end{aligned} \quad (14)$$

where $(\cdot)'$ indicates the derivative with respect to z .

Exploiting the domain structure (see Eq. (3)) it is possible to split the integral over the volume Ω into an integral over the middle-plane A and an integral within the thickness h . As a consequence we can rewrite Eq. (14) as:

$$\begin{aligned} \delta J_{HR} &:= \int_A (G_{jp} \delta \tilde{u}_j \bar{\mathbf{u}}_j \cdot \text{div}_A(\bar{\boldsymbol{\zeta}}_p \tilde{\zeta}_p) + G_{jr} \delta \tilde{u}_j \bar{\mathbf{u}}_j \cdot \bar{\boldsymbol{\tau}}_r \tilde{\tau}_r \\ &+ G_{lr} \delta \tilde{w}_l \text{div}_A(\bar{\boldsymbol{\tau}}_r \tilde{\tau}_r) + G_{lt} \delta \tilde{w}_l \tilde{\boldsymbol{\zeta}}_t) d\Omega \\ &+ \int_A (G_{qi} \text{div}_A(\delta \tilde{\zeta}_q \bar{\boldsymbol{\zeta}}_q) \cdot \bar{\mathbf{u}}_i \tilde{u}_i + G_{si} \delta \tilde{\tau}_s \bar{\boldsymbol{\tau}}_s \cdot \bar{\mathbf{u}}_i \tilde{u}_i \\ &+ G_{sk} \text{div}_A(\delta \tilde{\tau}_s \bar{\boldsymbol{\tau}}_s) \bar{\mathbf{w}}_k + G_{vk} \delta \tilde{\zeta}_v \bar{\mathbf{w}}_k) d\Omega \\ &+ \int_A (G_{qp} \delta \tilde{\zeta}_q \bar{\boldsymbol{\zeta}}_q : \mathbf{D}_{AA} : \bar{\boldsymbol{\zeta}}_p \tilde{\zeta}_p + G_{qr} \delta \tilde{\zeta}_q \bar{\boldsymbol{\zeta}}_q : \mathbf{D}_{A\tau} \cdot \bar{\boldsymbol{\tau}}_r \tilde{\tau}_r \\ &+ G_{qt} \delta \tilde{\zeta}_q \bar{\boldsymbol{\zeta}}_q : \mathbf{D}_{A\zeta} \tilde{\boldsymbol{\zeta}}_t + G_{sp} \delta \tilde{\tau}_s \bar{\boldsymbol{\tau}}_s \cdot \mathbf{D}_{\tau A} : \bar{\boldsymbol{\zeta}}_p \tilde{\zeta}_p \\ &+ G_{sr} \delta \tilde{\tau}_s \bar{\boldsymbol{\tau}}_s \cdot \mathbf{D}_{\tau\tau} \cdot \bar{\boldsymbol{\tau}}_r \tilde{\tau}_r + G_{st} \delta \tilde{\tau}_s \bar{\boldsymbol{\tau}}_s \cdot \mathbf{D}_{t\zeta} \tilde{\boldsymbol{\zeta}}_t \\ &+ G_{vp} \delta \tilde{\zeta}_v \mathbf{D}_{hA} : \bar{\boldsymbol{\zeta}}_p \tilde{\zeta}_p + G_{vr} \delta \tilde{\zeta}_v \mathbf{D}_{h\tau} \cdot \bar{\boldsymbol{\tau}}_r \tilde{\tau}_r + G_{vt} \delta \tilde{\zeta}_v \mathbf{D}_{hh} \tilde{\boldsymbol{\zeta}}_t) d\Omega \\ &+ \int_A (\delta \tilde{u}_j \bar{\mathbf{u}}_j \cdot \mathbf{F}_j + \delta \tilde{w}_l \bar{\mathbf{f}}_l) d\Omega \\ &- (\delta \tilde{\zeta}_q|_{\partial A} \bar{\boldsymbol{\zeta}}_q \cdot \mathbf{n}_A \cdot \bar{\mathbf{U}}_q + \delta \tilde{\tau}_s|_{\partial A} \bar{\boldsymbol{\tau}}_s \cdot \mathbf{n}_A \bar{\mathbf{W}}_s) dA = 0 \end{aligned} \quad (15)$$

where the coefficients are defined as follows:

We highlight that Eq. (15) can be seen as the weak formulation of the proposed plate-theory.

2.3. Partial differential equation derivation

In order to derive the 2D partial differential equations that govern the plate-theory, we need to apply the divergence theorem to the fifth and seventh terms of Eq. (15), as illustrated in the following.

$$\begin{aligned} \int_A G_{qi} \text{div}_A(\delta \tilde{\zeta}_q \bar{\boldsymbol{\zeta}}_q) \cdot \bar{\mathbf{u}}_i \tilde{u}_i dz &= G_{qi} \delta \tilde{\zeta}_q|_{\partial A} \bar{\boldsymbol{\zeta}}_q \cdot \mathbf{n}_A \cdot \bar{\mathbf{u}}_i \tilde{u}_i \\ &- \int_A G_{qi} \delta \tilde{\zeta}_q \bar{\boldsymbol{\zeta}}_q \cdot \text{grad}_A^s(\bar{\mathbf{u}}_i \tilde{u}_i) dz \\ &\times \int_A G_{sk} \text{div}_A(\delta \tilde{\tau}_s \bar{\boldsymbol{\tau}}_s) \bar{\mathbf{w}}_k dz \\ &= G_{sk} \delta \tilde{\tau}_s|_{\partial A} \bar{\boldsymbol{\tau}}_s \cdot \mathbf{n}_A \bar{\mathbf{w}}_k \\ &- \int_A G_{sk} \delta \tilde{\tau}_s \bar{\boldsymbol{\tau}}_s \text{grad}_A(\bar{\mathbf{w}}_k) dz \end{aligned} \quad (17)$$

where $\text{grad}_A^s(\bar{\mathbf{u}})$ is the symmetric gradient, defined as

$$\text{grad}_A^s(\bar{\mathbf{u}}) = \frac{1}{2} (\text{grad}_A(\bar{\mathbf{u}}) + \text{grad}_A^T(\bar{\mathbf{u}})) \quad (18)$$

Substituting Eqs. (17) and (15) can be rewritten as:

$$\begin{aligned} \delta J_{HR} := & \int_A (G_{jp} \delta \tilde{\mathbf{u}}_j \tilde{\mathbf{u}}_j \cdot \text{div}_A(\tilde{\mathbf{c}}_p \tilde{\zeta}_p) + G_{jr} \delta \tilde{\mathbf{u}}_j \tilde{\mathbf{u}}_j \cdot \tilde{\boldsymbol{\tau}}_r \tilde{\boldsymbol{\tau}}_r \\ & + G_{lr} \delta \tilde{\mathbf{w}}_l \text{div}_A(\tilde{\boldsymbol{\tau}}_r \tilde{\boldsymbol{\tau}}_r) + G_{lt} \delta \tilde{\mathbf{w}}_l \tilde{\zeta}_t) d\Omega \\ & + \int_A (-G_{qi} \delta \tilde{\zeta}_q \tilde{\zeta}_q \cdot \text{grad}_A^s(\tilde{\mathbf{u}}_i \tilde{\mathbf{u}}_i) + G_{si} \delta \tilde{\boldsymbol{\tau}}_s \tilde{\boldsymbol{\tau}}_s \cdot \tilde{\mathbf{u}}_i \tilde{\mathbf{u}}_i \\ & - G_{sk} \delta \tilde{\boldsymbol{\tau}}_s \tilde{\boldsymbol{\tau}}_s \cdot \text{grad}_A(\tilde{\mathbf{w}}_k) + G_{vk} \delta \tilde{\zeta}_v \tilde{\zeta}_v) d\Omega \\ & + \int_A (G_{qp} \delta \tilde{\zeta}_q \tilde{\zeta}_q : \mathbf{D}_{AA} : \tilde{\zeta}_p \tilde{\zeta}_p + G_{qr} \delta \tilde{\zeta}_q \tilde{\zeta}_q : \mathbf{D}_{Ar} : \tilde{\boldsymbol{\tau}}_r \tilde{\boldsymbol{\tau}}_r \\ & + G_{qt} \delta \tilde{\zeta}_q \tilde{\zeta}_q : \mathbf{D}_{At} : \tilde{\zeta}_t \tilde{\zeta}_t + G_{sp} \delta \tilde{\boldsymbol{\tau}}_s \tilde{\boldsymbol{\tau}}_s : \mathbf{D}_{tA} : \tilde{\zeta}_p \tilde{\zeta}_p \\ & + G_{sr} \delta \tilde{\boldsymbol{\tau}}_s \tilde{\boldsymbol{\tau}}_s : \mathbf{D}_{rt} : \tilde{\boldsymbol{\tau}}_r \tilde{\boldsymbol{\tau}}_r + G_{st} \delta \tilde{\boldsymbol{\tau}}_s \tilde{\boldsymbol{\tau}}_s : \mathbf{D}_{th} : \tilde{\zeta}_t \tilde{\zeta}_t \\ & + G_{vp} \delta \tilde{\zeta}_v \tilde{\zeta}_v : \mathbf{D}_{hA} : \tilde{\zeta}_p \tilde{\zeta}_p + G_{vr} \delta \tilde{\zeta}_v \tilde{\zeta}_v : \mathbf{D}_{hr} : \tilde{\boldsymbol{\tau}}_r \tilde{\boldsymbol{\tau}}_r + G_{vt} \delta \tilde{\zeta}_v \tilde{\zeta}_v : \mathbf{D}_{ht} : \tilde{\zeta}_t \tilde{\zeta}_t) d\Omega \\ & + \int_A (\delta \tilde{\mathbf{u}}_j \tilde{\mathbf{u}}_j \cdot \mathbf{F}_j + \delta \tilde{\mathbf{w}}_l F_l) d\Omega \\ & + \delta \tilde{\zeta}_q|_{\partial A} \tilde{\zeta}_q \cdot \mathbf{n}_A \cdot (G_{qi} \tilde{\mathbf{u}}_i \tilde{\mathbf{u}}_i - \tilde{\mathbf{U}}_q) \\ & + \delta \tilde{\boldsymbol{\tau}}_s|_{\partial A} \tilde{\boldsymbol{\tau}}_s \cdot \mathbf{n}_A (G_{sk} \tilde{\mathbf{w}}_k - \tilde{\mathbf{W}}_s) dA = 0 \end{aligned} \quad (19)$$

Since Eq. (19) must be satisfied for all virtual fields, the following partial differential equations must be satisfied in the middle-plane A:

$$G_{jp} \tilde{\mathbf{u}}_j \cdot \text{div}_A(\tilde{\mathbf{c}}_p \tilde{\zeta}_p) + G_{jr} \tilde{\mathbf{u}}_j \cdot \tilde{\boldsymbol{\tau}}_r \tilde{\boldsymbol{\tau}}_r + \tilde{\mathbf{u}}_j \cdot \mathbf{F}_j = \mathbf{0} \quad (20a)$$

$$G_{lr} \text{div}_A(\tilde{\boldsymbol{\tau}}_r \tilde{\boldsymbol{\tau}}_r) + G_{lt} \tilde{\zeta}_t + F_l = \mathbf{0} \quad (20b)$$

$$\begin{aligned} & - G_{qi} \tilde{\zeta}_q \cdot \text{grad}_A^s(\tilde{\mathbf{u}}_i \tilde{\mathbf{u}}_i) + G_{qp} \tilde{\zeta}_q : \mathbf{D}_{AA} : \tilde{\zeta}_p \tilde{\zeta}_p \\ & + G_{qr} \tilde{\zeta}_q : \mathbf{D}_{Ar} : \tilde{\boldsymbol{\tau}}_r \tilde{\boldsymbol{\tau}}_r + G_{qt} \tilde{\zeta}_q : \mathbf{D}_{At} : \tilde{\zeta}_t \tilde{\zeta}_t = \mathbf{0} \end{aligned} \quad (20c)$$

$$\begin{aligned} & G_{si} \tilde{\boldsymbol{\tau}}_s \cdot \tilde{\mathbf{u}}_i \tilde{\mathbf{u}}_i - G_{sk} \tilde{\boldsymbol{\tau}}_s \cdot \text{grad}_A(\tilde{\mathbf{w}}_k) + G_{sp} \tilde{\boldsymbol{\tau}}_s : \mathbf{D}_{tA} : \tilde{\zeta}_p \tilde{\zeta}_p \\ & + G_{sr} \tilde{\boldsymbol{\tau}}_s : \mathbf{D}_{rt} : \tilde{\boldsymbol{\tau}}_r \tilde{\boldsymbol{\tau}}_r + G_{st} \tilde{\boldsymbol{\tau}}_s : \mathbf{D}_{th} : \tilde{\zeta}_t \tilde{\zeta}_t = \mathbf{0} \end{aligned} \quad (20d)$$

$$G_{vk} \tilde{\mathbf{w}}_k + G_{vp} \mathbf{D}_{hA} : \tilde{\zeta}_p \tilde{\zeta}_p + G_{vr} \mathbf{D}_{hr} : \tilde{\boldsymbol{\tau}}_r \tilde{\boldsymbol{\tau}}_r + G_{vt} \mathbf{D}_{ht} : \tilde{\zeta}_t \tilde{\zeta}_t = \mathbf{0} \quad (20e)$$

together with the following boundary conditions that must be satisfied on the middle-plane boundary ∂A :

$$G_{qi} \tilde{\mathbf{u}}_i \tilde{\mathbf{u}}_i - \tilde{\mathbf{U}}_q = \mathbf{0} \quad (21a)$$

$$G_{sk} \tilde{\mathbf{w}}_k - \tilde{\mathbf{W}}_s = \mathbf{0} \quad (21b)$$

The partial differential Eqs. (20) and the boundary conditions (21) are the strong formulation of the plate-theory. In particular, we highlight the following statements.

- Eqs. (20a) and (20b) enforce the plate equilibrium. More in detail, Eq. (20a) enforces the membrane and the bending equilibrium whereas Eq. (20b) enforces the transversal equilibrium.
- Eqs. 20c, 20d, and 20e model the constitutive and the compatibility relations. In particular, Eq. (20e) represents only algebraic relations and, as a consequence, we can conclude that the plate theory (20) is governed by an algebraic-differential equations system.
- The assumption that the thickness shape functions are linearly independent ensures that it is possible to statically condensate out all the stress variables and obtain an hybrid version of the plate-theory. Nevertheless, this opportunity will not be investigated in the present document.
- The displacement boundary conditions (Eqs. (21a) and (21b)) are a natural outcome of the manipulation of the problem variational formulation.
- On the other hand, we recall that the boundary equilibrium equations are imposed in spaces definitions (5) and must be satisfied a priori by all the stresses involved in the problem formulation.
- Despite the heavy initial assumption on boundary displacements, the model leads in-plane and transversal boundary displacements to be managed separately.
- The number of boundary conditions depends on the number of adopted thickness shape-functions (specifically the boundary conditions result equal to $q + s$). As a consequence, using numerous thickness shape-functions, we are able to manage refined boundary conditions and situations e.g.

displacement distributions that induce only local effects. Nevertheless this model's capability will be investigated in the future.

- Using suitable assumptions on displacements thickness shape functions and opportunely substituting displacement boundary conditions with the dual conditions on stresses in all ∂A or only in some portion of it, it is also possible to obtain boundary conditions more usual in plate modeling (hinge, simple support, etc.).

2.4. FSDT equations recovery

In this subsection we show that is possible to recover classical FSDT equations using Eq. (20) and suitable assumptions on thickness shape functions.

Specifically, we assume that plate is homogeneous and made of an isotropic material characterized by a Young's modulo $E \neq 0$ and a vanishing Poisson's ratio $\nu = 0$. Moreover we assume that $\zeta_z = 0$ and we introduce the following thickness shape functions:

$$\begin{aligned} \hat{\mathbf{u}}_1 = \hat{\mathbf{u}}_2 = 1; \quad \hat{\mathbf{u}}_3 = \hat{\mathbf{u}}_4 = z; \quad \hat{\mathbf{w}}_1 = 1 \\ \hat{\boldsymbol{\tau}}_1 = \hat{\boldsymbol{\tau}}_2 = \left(1 - 4\frac{z^2}{h^2}\right); \quad \hat{\zeta}_1 = \hat{\zeta}_2 = \hat{\zeta}_3 = 1; \quad \hat{\zeta}_4 = \hat{\zeta}_5 = \hat{\zeta}_6 = z \end{aligned} \quad (22)$$

$$\begin{aligned} \tilde{\mathbf{u}}_1 = \tilde{\mathbf{u}}_3 = \{1, 0\}^T; \quad \tilde{\mathbf{u}}_2 = \tilde{\mathbf{u}}_4 = \{0, 1\}^T; \\ \tilde{\boldsymbol{\tau}}_1 = \{1, 0\}^T; \quad \tilde{\boldsymbol{\tau}}_2 = \{0, 1\}^T \end{aligned} \quad (23)$$

$$\tilde{\zeta}_1 = \tilde{\zeta}_4 = \begin{Bmatrix} 1 & 0 \\ 0 & 0 \end{Bmatrix}; \quad \tilde{\zeta}_2 = \tilde{\zeta}_5 = \begin{Bmatrix} 0 & 1 \\ 1 & 0 \end{Bmatrix}; \quad \tilde{\zeta}_3 = \tilde{\zeta}_6 = \begin{Bmatrix} 0 & 0 \\ 0 & 1 \end{Bmatrix}$$

and the corresponding coefficient functions, collected in suitable vectors:

$$\begin{aligned} \tilde{\mathbf{u}}_i = \{u_0, v_0, \varphi_x, \varphi_y\}^T; \quad \tilde{\mathbf{w}}_k = w_0; \quad \tilde{\zeta}_p \\ = \{\sigma_{x0}, \sigma_{y0}, \tau_{xy0}, \sigma_{x1}, \sigma_{y1}, \tau_{xy1}\}^T; \quad \tilde{\boldsymbol{\tau}}_r = \{\tau_{xz}, \tau_{yz}\}^T \end{aligned} \quad (24)$$

In consequence of the so far introduced assumptions it results that $\tilde{\zeta}_t = 0$ and $\mathbf{D}_{Ar} = \mathbf{0}$, and Eq. (20e) becomes the trivial identity $\mathbf{0} = \mathbf{0}$. Moreover, the coefficient G could be easily evaluated and we resume their values in the following matrices:

$$\begin{aligned} G_{jp} = \begin{Bmatrix} \bar{h} & \bar{h} & \bar{h} & 0 & 0 & 0 \\ \bar{h} & \bar{h} & \bar{h} & 0 & 0 & 0 \\ 0 & 0 & 0 & J & J & J \\ 0 & 0 & 0 & J & J & J \end{Bmatrix}; \quad G_{jr} = \frac{2}{3} \begin{Bmatrix} 0 & 0 \\ 0 & 0 \\ \bar{h} & \bar{h} \\ \bar{h} & \bar{h} \end{Bmatrix}; \quad G_{lr} = \frac{2}{3} \{\bar{h}; \bar{h}\} \\ G_{qp} = \begin{Bmatrix} \bar{h} & \bar{h} & \bar{h} & 0 & 0 & 0 \\ \bar{h} & \bar{h} & \bar{h} & 0 & 0 & 0 \\ \bar{h} & \bar{h} & \bar{h} & 0 & 0 & 0 \\ 0 & 0 & 0 & J & J & J \\ 0 & 0 & 0 & J & J & J \\ 0 & 0 & 0 & J & J & J \end{Bmatrix}; \quad G_{sr} = \frac{8}{15} \begin{Bmatrix} \bar{h} & \bar{h} \\ \bar{h} & \bar{h} \end{Bmatrix} \end{aligned} \quad (25)$$

where $J = \bar{h}^3/12$.

Assuming also a vanishing load, i.e. $\mathbf{f} = \mathbf{0}$, Eqs. (20) reduce to the following scalar equations:

$$\bar{h} \sigma_{x0,x} + \bar{h} \tau_{xy0,y} = 0 \quad (26a)$$

$$\bar{h} \tau_{xy0,x} + \bar{h} \sigma_{y0,y} = 0 \quad (26b)$$

$$J \sigma_{x1,x} + J \tau_{xy1,y} - \frac{2}{3} \bar{h} \tau_{xz} = 0 \quad (26c)$$

$$J \tau_{xy1,x} + J \sigma_{y1,y} - \frac{2}{3} \bar{h} \tau_{yz} = 0 \quad (26d)$$

$$\frac{2}{3} \bar{h} \tau_{xz,x} = 0 \quad (26e)$$

$$\frac{2}{3} \bar{h} \tau_{yz,y} = 0 \quad (26f)$$

$$-\bar{h}u_{0,x} + \frac{\bar{h}}{E}\sigma_{x0} = 0 \quad (26g)$$

$$-\bar{h}u_{0,y} - \bar{h}v_{0,x} + \frac{2\bar{h}}{E}\tau_{xy0} = 0 \quad (26h)$$

$$-\bar{h}v_{0,y} + \frac{\bar{h}}{E}\sigma_{y0} = 0 \quad (26i)$$

$$-J\varphi_{x,x} + \frac{J}{E}\sigma_{x1} = 0 \quad (26j)$$

$$-J\varphi_{x,y} - J\varphi_{y,x} + \frac{2J}{E}\tau_{xy1} = 0 \quad (26k)$$

$$-J\varphi_{y,y} + \frac{J}{E}\sigma_{y1} = 0 \quad (26l)$$

$$\frac{2}{3}\bar{h}\varphi_x - \frac{2}{3}\bar{h}w_{0,x} + \frac{8}{15}\frac{2\bar{h}}{E}\tau_{xz} = 0 \quad (26m)$$

$$\frac{2}{3}\bar{h}\varphi_y - \frac{2}{3}\bar{h}w_{0,y} + \frac{8}{15}\frac{2\bar{h}}{E}\tau_{yz} = 0 \quad (26n)$$

Furthermore, using Equations from (26g)–(26m) and (26n) it is possible to express stress unknowns as a function of displacements. Substituting these latter expressions in Equations from (26a)–(26e) and (26f) we obtain the following problem displacement-formulation:

$$\bar{h}Eu_{0,xx} + \bar{h}\frac{E}{2}(u_{0,yy} + v_{0,xy}) = 0 \quad (27a)$$

$$\bar{h}\frac{E}{2}(u_{0,xy} + v_{0,xx}) + \bar{h}Ev_{0,yy} = 0 \quad (27b)$$

$$J\varphi_{x,xx} + J\frac{E}{2}(\varphi_{x,yy} + \varphi_{y,xy}) - \frac{5}{6}\frac{E}{2}\bar{h}(w_{0,x} - \varphi_x) = 0 \quad (27c)$$

$$J\varphi_{y,yy} + J\frac{E}{2}(\varphi_{x,xy} + \varphi_{y,xx}) - \frac{5}{6}\frac{E}{2}\bar{h}(w_{0,y} - \varphi_y) = 0 \quad (27d)$$

$$\frac{5}{6}\frac{E}{2}\bar{h}(w_{0,xx} - \varphi_{x,x}) = 0 \quad (27e)$$

$$\frac{5}{6}\frac{E}{2}\bar{h}(w_{0,yy} - \varphi_{y,y}) = 0 \quad (27f)$$

We highlight that in Equations from (27c)–(27e) and (27f) the shear factor 5/6 appears naturally from the problem formulation, without the need of any further evaluation or discussion.

3. Simply supported plate

In the following we focus on the case of a rectangular plate for which, due to the simple geometry, it is possible to easily compute a series solution. Moreover, we assume that the plate is simply supported along its edges, i.e.:

$$\int_{-\frac{\bar{h}}{2}}^{\frac{\bar{h}}{2}} u(x, y, z)|_{y=0,b} dz = 0; \quad \int_{-\frac{\bar{h}}{2}}^{\frac{\bar{h}}{2}} v(x, y, z)|_{x=0,a} dz = 0; \quad \int_{-\frac{\bar{h}}{2}}^{\frac{\bar{h}}{2}} w(x, y, z)|_{\partial A} dz = 0 \quad (28)$$

Finally, we assume that the load is orthogonal to the plate middle-plane (i.e. $\mathbf{f} = \{0, 0, f_z\}^T$) and it could have a uniform distribution. All the assumptions introduced so far allow the analytical solution of many different theories to be evaluated.

In particular, to compare the proposed theory with some others, in the following we provide the details necessary to evaluate the analytical solutions for CPT, FSDT, elasticity theory, and the theory proposed in the Current Work and represented by Eq. (20).

3.1. Classical plate theory

CPT solution is completely determined by the displacement of the points on the middle-plane along the three coordinate directions as:

$$u(x, y, z) = u_0(x, y) - z\frac{\partial w_0}{\partial x} \quad (29)$$

$$v(x, y, z) = v_0(x, y) - z\frac{\partial w_0}{\partial y}$$

$$w(x, y, z) = w_0(x, y)$$

where u_0 , v_0 , and w_0 are displacement field of middle-plane along x , y , and z directions, respectively. We notice that the assumed displacement fields lead to a vanishing transverse strains (i.e. $\gamma_{xz} = \gamma_{yz} = 0$). Due to the assigned boundary conditions and load, u_0 and v_0 are going to be always equal to zero and we will neglect them in the following.

On the other hand, we use a double sin series with unknown coefficients W_{mn} in order to describe the vertical displacement field w_0 , as illustrated in the following.

$$w_0(x, y) = \sum_{n=1}^{\infty} \sum_{m=1}^{\infty} W_{mn} \sin\left(\frac{m\pi}{a}x\right) \sin\left(\frac{n\pi}{b}y\right) \quad (30)$$

Analogously, the load could be expressed as a double sin series:

$$q(x, y) = \sum_{n=1}^{\infty} \sum_{m=1}^{\infty} Q_{mn} \sin\left(\frac{m\pi}{a}x\right) \sin\left(\frac{n\pi}{b}y\right) \quad (31)$$

where Q_{mn} can be determined with:

$$Q_{mn} = \frac{4}{ab} \int_0^a \int_0^b \left(\int_{-\frac{\bar{h}}{2}}^{\frac{\bar{h}}{2}} f_z(x, y, z) dz \right) \sin\left(\frac{m\pi}{a}x\right) \sin\left(\frac{n\pi}{b}y\right) dx dy \quad (32)$$

The resulting bending moments M_{xx} , M_{yy} , and M_{xy} are obtained by introducing Eq. (30) in the compatibility relation $\boldsymbol{\varepsilon} = \nabla^s \mathbf{s}$, substituting the obtained strains $\boldsymbol{\varepsilon}$ into the constitutive relation $\boldsymbol{\sigma} = \mathbf{D}^{-1} \boldsymbol{\varepsilon}$, and evaluating the following integrals:

$$\begin{bmatrix} M_{xx} \\ M_{yy} \\ M_{xy} \end{bmatrix} = \int_{-\frac{\bar{h}}{2}}^{\frac{\bar{h}}{2}} \begin{bmatrix} z\sigma_{xx} \\ z\sigma_{yy} \\ z\tau_{xy} \end{bmatrix} dz \quad (33)$$

The analytical solution of CPT comes from the satisfaction of the following governing equation:

$$\frac{\partial^2}{\partial x^2} M_{xx} + 2\frac{\partial^2}{\partial x \partial y} M_{xy} + \frac{\partial^2}{\partial y^2} M_{yy} + q = 0 \quad (34)$$

We highlight that, due to the introduction of assumptions (30), (31) and (34) reduces to a set of infinite algebraic equations in infinite unknowns. Truncating both the double sin series (30) and (31) at suitable n and m , it is possible to evaluate numerically an approximation of the analytical solution. The complete solution procedure can be found in reference books [e.g. 7,45].

3.2. First order shear deformation theory

FSDT allows independent and arbitrary rotations of transverse segments of the plate, as described in the following:

$$\begin{aligned} u(x, y, z) &= u_0(x, y) - z\varphi_x(x, y) \\ v(x, y, z) &= v_0(x, y) - z\varphi_y(x, y) \\ w(x, y, z) &= w_0(x, y) \end{aligned} \quad (35)$$

As in Section 3.1, u_0 , v_0 , and w_0 denote the middle-plane displacements whereas φ_x and φ_y denote the rotations of a transverse normal around the y and x axes respectively.

In addition to the double sin series expansion introduced in Eqs. (30) and (31), we use 2 sin-cos series with unknown coefficients φ_{mn}^x and φ_{mn}^y , in order to describe the rotations φ_x and φ_y respectively, as illustrated in the following.

$$\begin{aligned} \varphi_x(x, y) &= \sum_{n=1}^{\infty} \sum_{m=1}^{\infty} \phi_{mn}^x \cos\left(\frac{m\pi}{a}x\right) \sin\left(\frac{n\pi}{b}y\right) \\ \varphi_y(x, y) &= \sum_{n=1}^{\infty} \sum_{m=1}^{\infty} \phi_{mn}^y \sin\left(\frac{m\pi}{a}x\right) \cos\left(\frac{n\pi}{b}y\right) \end{aligned} \quad (36)$$

As a consequence of Eq. (35), the transverse shears strains and the corresponding stresses result to be constant through the plate thickness, whereas in order to satisfy boundary equilibrium they must vanish at boundaries $z = \pm \frac{h}{2}$. As a consequence, we introduce shear correction factor $K_s = 5/6$, with the aim to compute the correct amount of deformation work induced by shear deformations.

The resulting shear forces Q_x and Q_y could be obtained evaluating the following integrals:

$$\begin{Bmatrix} Q_x \\ Q_y \end{Bmatrix} = K_s \int_{-\frac{h}{2}}^{\frac{h}{2}} \begin{Bmatrix} \tau_{xz} \\ \tau_{yz} \end{Bmatrix} dz \quad (37)$$

where the shear stresses τ_{xz} and τ_{yz} are evaluated through the procedure introduced in Section 3.1.

The analytical solution of FSDT comes from the satisfaction of the following governing equations:

$$\begin{aligned} \frac{\partial Q_x}{\partial x} + \frac{\partial Q_y}{\partial y} + q &= 0 \\ \frac{\partial M_{xx}}{\partial x} + \frac{\partial M_{xy}}{\partial y} - Q_x &= 0 \\ \frac{\partial M_{xy}}{\partial x} + \frac{\partial M_{yy}}{\partial y} - Q_y &= 0 \end{aligned} \quad (38)$$

Similarly to CPT, due to the introduction of assumptions (30), (36), (31) and (38) reduces to a set of infinite algebraic equations in infinite unknowns. Truncating the series (30), (36), and (31) at suitable n and m , it is possible to evaluate numerically an approximation of the analytical solution. Further details can be found in reference book [45].

3.3. Elasticity theory

As it is mentioned in Section 1, Pagano [39] studies the 3D solution for a rectangular simply supported plate. The 3D elasticity solution is based on the displacement field prediction. In particular Pagano [39] suggests the following expansion for the displacement field.

$$\begin{aligned} u(x, y, z) &= \sum_{n=1}^{\infty} \sum_{m=1}^{\infty} U(z) \cos\left(\frac{m\pi}{a}x\right) \sin\left(\frac{n\pi}{b}y\right) \\ v(x, y, z) &= \sum_{n=1}^{\infty} \sum_{m=1}^{\infty} V(z) \sin\left(\frac{m\pi}{a}x\right) \cos\left(\frac{n\pi}{b}y\right) \\ w(x, y, z) &= \sum_{n=1}^{\infty} \sum_{m=1}^{\infty} W(z) \sin\left(\frac{m\pi}{a}x\right) \sin\left(\frac{n\pi}{b}y\right) \end{aligned} \quad (39)$$

By using the 3D problem governing equations together with assumptions (39) and the boundary equilibrium on the top and bottom of the plate, the unknown functions along the z axis can be determined as illustrated in the reference paper.

3.4. Current work

In order to choose the thickness shape functions $\hat{\gamma}$, we need to recall the spaces where we choose both solution and virtual functions for the starting 3D problem (5). Furthermore, in order to ensure that the theory proposed in Section 2.3 is well-posed, Auricchio et al. [46] suggest to require the following condition:

$$\text{div}(S) = W \quad (40)$$

Moreover, we assume that the thickness shape functions $\hat{\gamma}$ are complete polynomial, defined by their maximum degree, denoted as $\text{deg}(\hat{\gamma})$. As a consequence, in order to satisfy Eq. (40), we need to enforce the following condition on thickness shape functions:

$$\begin{aligned} \text{deg}(\hat{\zeta}_p) &= \text{deg}(\hat{\tau}_r) - 1 = \text{deg}(\hat{u}_i) \\ \text{deg}(\hat{\tau}_r) &= \text{deg}(\hat{\zeta}_t) - 1 = \text{deg}(\hat{w}_k) \end{aligned} \quad (41)$$

Choosing $\text{deg}(\hat{\tau}_r) = 2$, in order to recover a shear distribution similar to the analytical solution, enforcing all the Eq. (41) and imposing boundary equilibrium (i.e. the essential condition) on $\partial\Omega_z$ we select the degrees of each scalar component as specified in Table 1.

We highlight the following statements.

- Displacement components u , v , and w are z -discontinuous. This assumption apparently violates the interlayer compatibility that nevertheless is naturally enforced by the plate theory Eqs. (20), according to the initial problem formulation (6).
- The in-plane stress components σ_x , σ_y , and τ_{xy} are z -discontinuous. This assumption appears as a reasonable choice with respect to initial problem formulation (6) since these stress-components has no role in interlayer equilibrium. Furthermore, from a physical point of view, assuming inhomogeneous plates the these stresses may be discontinuous within the thickness.
- The out-of-plane shear-stress components τ_{xz} and τ_{yz} and the out-of-plane stress σ_z are z -continuous. This assumption ensures that interlayer equilibrium is imposed as essential condition for the plate theory, according to the initial problem formulation (6).

As a consequence, the current work theory privileges an accurate stress description, according to the goals introduced at the end of Section 1 and it does not show inconsistencies with respect to the initial 3D problem formulation.

Using for each \hat{w}_i an expansion similar to the one introduced in Eq. (30), for each \hat{u}_i expansions similar to the ones introduced in Eq. (36), and the following expansions for stress coefficient functions, we can reduce the strong formulation of the plate theory (20) to a set of algebraic equations, as in all the previously discussed theories.

$$\begin{aligned} \tilde{\sigma}_i &= \sum_{n=1}^{\infty} \sum_{m=1}^{\infty} S_{mn}^i \cos\left(\frac{m\pi}{a}x\right) \sin\left(\frac{n\pi}{b}y\right) \quad i = x, y, z \\ \tilde{\tau}_{xy} &= \sum_{n=1}^{\infty} \sum_{m=1}^{\infty} S_{mn}^{xy} \cos\left(\frac{m\pi}{a}x\right) \cos\left(\frac{n\pi}{b}y\right) \\ \tilde{\tau}_{xz} &= \sum_{n=1}^{\infty} \sum_{m=1}^{\infty} S_{mn}^{xz} \cos\left(\frac{m\pi}{a}x\right) \sin\left(\frac{n\pi}{b}y\right) \\ \tilde{\tau}_{yz} &= \sum_{n=1}^{\infty} \sum_{m=1}^{\infty} S_{mn}^{yz} \sin\left(\frac{m\pi}{a}x\right) \cos\left(\frac{n\pi}{b}y\right) \end{aligned} \quad (42)$$

Table 1

Thickness shape functions: definition of polynomial degrees, z -continuity properties and resulting number of degree of freedom.

| | | Deg | Z-continuity | Layer DOF | Global DOF |
|----------|-------------|-----|--------------|-----------|------------|
| u | u | 1 | no | 2 | 2n |
| | v | 1 | no | 2 | 2n |
| w | w | 2 | no | 3 | 3n |
| | ζ | | | | |
| ζ | σ_x | 1 | no | 2 | 2n |
| | σ_y | 1 | no | 2 | 2n |
| | τ_{xy} | 1 | no | 2 | 2n |
| τ | σ_z | 3 | yes | 4 | 3n-1 |
| | τ_{xz} | 2 | yes | 3 | 2n-1 |
| | τ_{yz} | 2 | yes | 3 | 2n-1 |

3.5. Remarks on theories analytical solutions

We conclude this section highlighting the following remarks on the illustrated theories and the corresponding analytical solutions.

- The analytic solutions of all the presented theories can be numerically evaluated through a suitable truncation of the series expansions and solving numerically the obtained algebraic equations.
- All the series expansions are defined in a way that satisfy the boundary conditions (28).
- CPT and FSDT are *single-layer* models, i.e. they use functions globally defined on the whole thickness.
- On the other hand, elasticity theory and the Current Work are *layer-wise* models, i.e., considering multilayer plates, they could use functions defined locally on each layer.

4. Numerical results

In this section we compare the theories introduced in Section 3 through the discussion of some numerical results with the aim to highlight capabilities and limitations of the proposed modeling approach. In particular, we consider an homogeneous and isotropic plate and some multilayer orthotropic plates, which numerical results are discussed in SubSections 4.1 and 4.2 respectively. We highlight that, since the plate analytical solution is available only for orthotropic materials [39], we are forced to limit our attention on the restrictive hypothesis so far mentioned in order to perform a rigorous discussion. Nevertheless, the proposed theory can be applied to more general cases which rigorous investigation will be object of further developments.

In the following we consider the dimensionless transversal displacement evaluated at center of plate and defined as:

$$\bar{w} = \frac{Eh^3}{q_0 a^4} \left(\int_{-\frac{h}{2}}^{\frac{h}{2}} w \left(\frac{a}{2}, \frac{b}{2}, z \right) dz \right) \cdot 10^2 \tag{43}$$

where q_0 is the magnitude of uniformly distributed load or the maximum magnitude of the sinusoidally distributed load.

4.1. Isotropic plate

Table 2 reports the dimensionless transverse displacement \bar{w} evaluated for an isotropic square plate under uniform load. The parameter is evaluated considering the different theories introduced in Section 3, different series truncations, and different

Table 2
Dimensionless transversal displacement \bar{w} evaluated for one layer, isotropic, square, and simply supported plate, evaluate considering different theories, truncation terms, and span-to-depth ratios.

| Theory | n, m | $\frac{a}{h} = 5$ | $\frac{a}{h} = 10$ | $\frac{a}{h} = 20$ | $\frac{a}{h} = 50$ | $\frac{a}{h} = 100$ |
|--------------|----------|-------------------|--------------------|--------------------|--------------------|---------------------|
| CPT | n = m=10 | 4.5703 | 4.5703 | 4.5703 | 4.5703 | 4.5703 |
| | n = m=20 | 4.5701 | 4.5701 | 4.5701 | 4.5701 | 4.5701 |
| | n = m=30 | 4.5701 | 4.5701 | 4.5701 | 4.5701 | 4.5701 |
| FSDT | n = m=10 | 5.4558 | 4.7917 | 4.6256 | 4.5791 | 4.5725 |
| | n = m=20 | 5.4540 | 4.7911 | 4.6254 | 4.5790 | 4.5724 |
| | n = m=30 | 5.4543 | 4.7912 | 4.6254 | 4.5790 | 4.5724 |
| | n = m=40 | 5.4542 | 4.7912 | - | - | - |
| | n = m=50 | 5.4542 | - | - | - | - |
| Current Work | n = m=10 | 5.4638 | 4.7939 | 4.6262 | 4.5792 | 4.5725 |
| | n = m=20 | 5.4622 | 4.7933 | 4.6260 | 4.5791 | 4.5724 |
| | n = m=30 | 5.4623 | 4.7934 | 4.6260 | 4.5791 | 4.5724 |
| | n = m=40 | 5.4623 | 4.7934 | - | - | - |
| Elasticity | n = m=10 | 5.3654 | 4.7704 | 4.6204 | 4.5783 | 4.5723 |
| | n = m=20 | 5.3646 | 4.7700 | 4.6202 | 4.5782 | 4.5721 |
| | n = m=30 | 5.3646 | 4.7700 | 4.6202 | 4.5782 | 4.5721 |

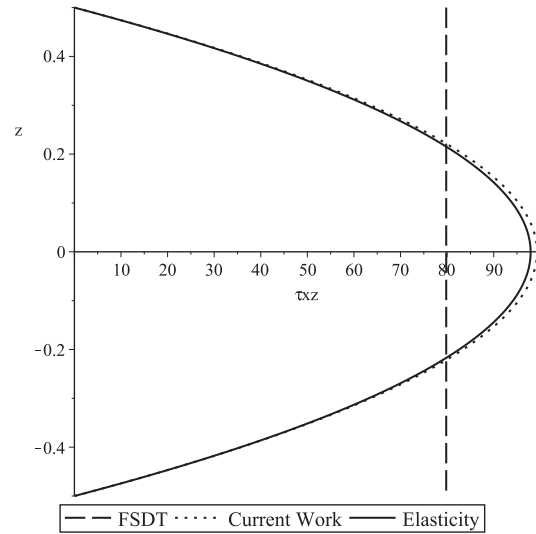


Fig. 3. Out of plane shear stress τ_{xz} evaluated for one layer, isotropic, square, and simply supported plate, distribution along the thickness evaluated in $(x, y) = (0, b/2)$.

span-to-depth ratios. Finally, we assume $K_s = 5/6$ as shear correction factor for FSDT.

We notice that the solutions converge with a number of expansion terms between 20 and 40 for all the considered theories and span-to-depth ratios. In particular, the convergence is quick for thin plates ($\frac{a}{h} = 100$ and $\frac{a}{h} = 50$) whereas it is slow for thick plates ($\frac{a}{h} = 5$ and $\frac{a}{h} = 10$). Focusing our attention to the theory proposed in Current Work, we notice that it converges faster than FSDT for $\frac{a}{h} = 5$. Moreover, the Current Work solution is not significantly different from FSDT for all the span-to-depth ratios, maybe as a consequence of the simple geometry and material properties that, among other consequences, lead the applied shear factor to be exact. Finally, for thin plate ($\frac{a}{h} = 100$), the solutions of current theory, elasticity, FSDT, and CPT are very close, as expected from theoretical analysis [2]. All the results reported in the following of this section are obtained using a number of expansion terms sufficient to ensure the convergence of the solution, according to the results reported in Table 2.

Fig. 3 shows the distribution of shear stress τ_{xz} along the thickness, evaluated in $(x, y) = (0, b/2)$. In particular, for the FSDT we plot the shear stress distribution evaluated using the compatibility and constitutive laws, using only those elements FSDT does not provide the correct shear stress distribution but it provides only its mean value, as noticed also in reference books [45]. On the other hand, it is well known that the equilibrium equation allows an accurate distribution of the shear stresses to be derived in FSDT. Specifically, it is possible to recover the quadratic distribution of the shear stress post-processing the in plane stress solution. For the homogeneous plate considered in this section, the shear stress distribution obtained through the equilibrium-equation post-processing is exactly equal to the one determined from the proposed approach.

Nevertheless, we notice that the Current Work theory is extremely accurate in predicting both the displacement and the stress distributions, without the need to introduce any shear correction factor or to perform any post-processing analysis.

4.2. Layered orthotropic plate

In this section we consider a multilayer plate, in which each layer is made of an orthotropic material with the following mechanical properties:

Table 3

Dimensionless transversal displacement \bar{w} evaluated for multi-layer, non-homogeneous, orthotropic, square, and simply supported plate, evaluate considering different theories, span-to-depth ratios and uniform load.

| | Theory | $\frac{a}{h} = 5$ | $\frac{a}{h} = 10$ | $\frac{a}{h} = 20$ | $\frac{a}{h} = 50$ | $\frac{a}{h} = 100$ |
|----------|--------------|-------------------|--------------------|--------------------|--------------------|---------------------|
| 1 Layer | CPT | 0.8187 | 0.8187 | 0.8187 | 0.8187 | 0.8187 |
| | FSDT | 1.9183 | 1.0776 | 0.8595 | 0.7977 | 0.7888 |
| | Current Work | 1.9373 | 1.0900 | 0.8698 | 0.8073 | 0.7984 |
| | Elasticity | 1.9008 | 1.0852 | 0.8689 | 0.8072 | 0.7983 |
| 2 Layers | CPT | 2.0439 | 2.0439 | 2.0439 | 2.0439 | 2.0439 |
| | FSDT | 2.8570 | 2.1006 | 1.9119 | 1.8592 | 1.8516 |
| | Current Work | 2.8733 | 2.1451 | 1.9630 | 1.9121 | 1.9048 |
| | Elasticity | 2.8362 | 2.1370 | 1.9611 | 1.9118 | 1.9047 |
| 3 Layers | CPT | 0.8342 | 0.8342 | 0.8342 | 0.8342 | 0.8342 |
| | FSDT | 2.0923 | 1.1434 | 0.8873 | 0.8136 | 0.8030 |
| | Current Work | 2.4872 | 1.2925 | 0.9366 | 0.8308 | 0.8155 |
| | Elasticity | 2.4611 | 1.2882 | 0.9357 | 0.8307 | 0.8154 |
| 4 Layers | CPT | 0.8485 | 0.8485 | 0.8485 | 0.8485 | 0.8485 |
| | FSDT | 2.0613 | 1.1507 | 0.8998 | 0.8267 | 0.8161 |
| | Current Work | 2.4139 | 1.2838 | 0.9459 | 0.8442 | 0.8293 |
| | Elasticity | 2.3905 | 1.2795 | 0.9450 | 0.8440 | 0.8293 |

Table 4

Displacement errors evaluated for multi-layer, non-homogeneous, orthotropic, square, and simply supported plate, evaluate considering different theories, span-to-depth ratios and a uniform load.

| Error(%) | Theory | $\frac{a}{h} = 5$ | $\frac{a}{h} = 10$ | $\frac{a}{h} = 20$ | $\frac{a}{h} = 50$ | $\frac{a}{h} = 100$ |
|----------|--------------|-------------------|--------------------|--------------------|--------------------|---------------------|
| 1 Layer | CPT | 56.929 | 24.558 | 5.7774 | 1.4247 | 2.5554 |
| | FSDT | 0.9207 | 0.7003 | 1.0818 | 1.1769 | 1.1900 |
| | Current Work | 1.9202 | 0.4423 | 0.1036 | 0.0124 | 0.0125 |
| 2 Layers | CPT | 27.935 | 4.3566 | 4.2221 | 6.9097 | 7.3082 |
| | FSDT | 0.7334 | 1.7033 | 2.5088 | 2.7513 | 2.7878 |
| | Current Work | 1.3081 | 0.3790 | 0.0969 | 0.0157 | 0.0053 |
| 3 Layers | CPT | 66.105 | 35.243 | 10.848 | 0.4213 | 2.3056 |
| | FSDT | 14.985 | 11.241 | 5.1726 | 2.0585 | 1.5207 |
| | Current Work | 1.0605 | 0.3338 | 0.0962 | 0.0120 | 0.0123 |
| 4 Layers | CPT | 64.505 | 33.685 | 10.212 | 0.5332 | 2.3152 |
| | FSDT | 13.771 | 10.066 | 4.7831 | 2.0498 | 1.5917 |
| | Current Work | 0.9789 | 0.3361 | 0.0952 | 0.0237 | $< 10^{-4}$ |

$$\begin{aligned}
 E_1 &= 25 \cdot E_2; & E_2 &= E_3 \\
 G_{12} &= G_{13} = 0.5 \cdot E_2; & G_{23} &= 0.2 \cdot E_2 \\
 \nu_{12} &= \nu_{13} = \nu_{23} = 0.25
 \end{aligned}
 \tag{44}$$

More in detail, we consider plates made of 2, 3, and 4 equal layers with the fibers orientated as follows: 0/90, 0/90/0, and 0/90/90/0 respectively. As usual in engineering practice the numbers indicate the orientation angle of the fibers in each layer.

Table 3 reports the dimension-less transversal displacement evaluated for a square, simply supported, and uniformly loaded plates with different number of layers and different span-to-depth ratios.

We notice that CPT theory provide a reasonable prediction only for slender plates ($\frac{a}{h} = 50$ and $\frac{a}{h} = 100$), whereas its solution effectiveness worsen quickly decreasing the span-to-depth ratio.

In order to discuss more rigorously the results of Table 3, we introduce also the displacement relative error, defined as:

$$error = \frac{W_i - W_{elasticity}}{W_{elasticity}} \times 100 \quad i = CPT, FSDT, \text{ and Current Work}
 \tag{45}$$

Table 4 reports the relative errors evaluated for the theories considered in this paper and for the multilayer plate. We notice the following statements.

- Increasing the number of layers, CPT and FSDT becomes ineffective in predicting the maximum displacement, also for relatively slender plates ($\frac{a}{h} = 20$).
- On the other hand, the Current Work relative error remains $< 1\%$ independently from the number of layers and the span-to-depth ratio.
- Moreover, looking at the 4 layer relative errors we observe that increasing the span-to-depth ratio of 1 order of magnitude, the relative errors of CPT and FSDT decrease of 1 order of magnitude whereas the Current Work relative error decrease of more than 4 order of magnitude.

Fig. 4 plots the out of plane shear stresses for the 3 layers plate so far introduced. The figure confirm that, also in complex

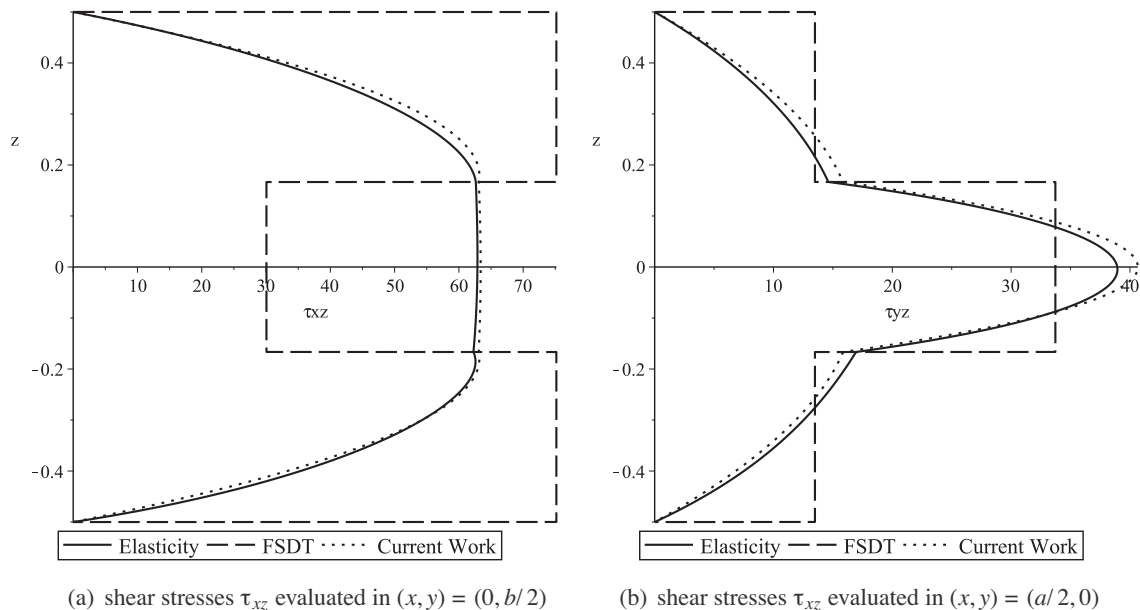


Fig. 4. Out of plane shear stresses τ_{xz} and τ_{yz} evaluated for 3 layers, non homogeneous, orthotropic, square, and simply supported plate, fiber orientation 0/90/0, distribution along the thickness.

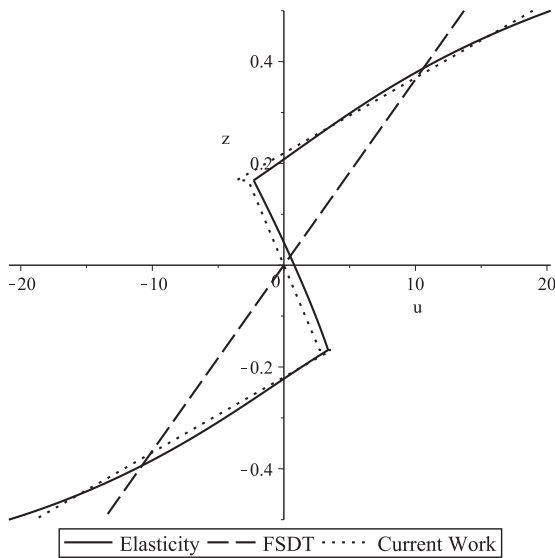


Fig. 5. In-plane displacement u evaluated for 3 layers, non homogeneous, orthotropic, square, and simply supported plate, fiber orientation $0/90/0$, distribution along the thickness.

situations, the Current Work provides accurate stress descriptions without the need of any post-processing operation.

Fig. 5 plots the out of plane shear stresses for 3 layers plate so far introduced. The figure highlight that FSDT has only the capability to catch the displacement mean values (membrane displacement and rotation). On the contrary, the Current Work has the capability to predict effectively also complex displacement distributions, leading to extremely accurate description of multilayer plate behavior and opening interesting perspective for enhanced analysis.

5. Conclusions

This paper considers a new modeling approach applicable to inhomogeneous, anisotropic, and moderately thick plates based on HR principle and dimension reduction method. More in detail, we start choosing an expression of the HR principle that privileges an accurate description of stress field. We continue reducing the problem dimension, i.e. we approximate each field variable as a combination of some assigned cross section shape functions weighted with arbitrary coefficient functions that become the plate model unknowns. Finally, we obtain the system of partial differential equations governing the plate behavior through some analytical calculations. In order to understand the capabilities of Current Work, we compare the current-work analytical solution with the analytical solutions of other well known theories available in literature.

The main advantages of the proposed theory are listed in the following.

- As a consequence of the use of the HR principle, the obtained theory consider separately displacements and stresses.
- Moreover, the use of the HR principle dual formulation leads stresses to be described more accurately than displacements, allowing the goal of an accurate stress description to be achieved increasing only useful variables.
- The approach used to obtain the plate-theory allows the number of unknown variables to use within the equations to be chosen, opening the possibility to manage both theory accuracy and costs.

- The proposed approach does not need the introduction of shear correction factor, at least adopting the assumptions introduced in this paper.
- Stresses are obtained directly from the theory, without the need of any post-processing operation.

The numerical results highlight the capability of the proposed theory to provide accurate solutions even in complex situations like inhomogeneous, orthotropic, and moderately thick plates. In particular, the performances of the proposed theory are equivalent to the performance of classical theories in predicting the plate maximum displacement for simple plate geometries. On the other hand, the proposed theory exceeds classical theories in predicting displacements for complex and/or thick plates. Moreover, the proposed theory results effective in the description of both displacement and stress distributions, catching complex behaviors like non-linear displacement distributions. Finally, numerical results highlight that the Current Work performances are not influenced by the number of layers.

Further investigations will include the development of the plate finite element corresponding to the proposed theory and the investigation of further aspects like stress concentration, local effects, buckling, dynamics, large deformations, and failure.

References

- [1] Reddy JN. *Mechanics of Laminated Composite Plates and Shells: Theory and Analysis*. CRC Press; 2004. ISBN 9780849315923.
- [2] Ciarlet PG. *Theory of Plates*. In: *Number Volume 2 in Studies in Mathematics and its Applications*. Elsevier Science; 1997. ISBN 9780080535913.
- [3] Reddy JN, Wang CM, Lee KH. *Shear Deformable Beams and Plates*. UK: Elsevier; 2000.
- [4] Whitney JM. Shear correction factor for orthotropic laminates under static load. *J Appl Mech* 1973;40(1):302–4.
- [5] Noor AK, Burton WS. Assessment of computational models for multilayered anisotropic plates. *Compos Struct* 1990;14(3):233–65.
- [6] Auricchio F, Sacco E. Refined first-order shear deformation theory models for composite laminates. *J Appl Mech* 2003;70:381–90.
- [7] Reddy JN. *Energy Principles and Variational Methods in Applied Mechanics*. Wiley; 2002. ISBN 9780471179856.
- [8] Carrera E. Theories and finite elements for multilayered, anisotropic, composite plates and shells. *Arch Comput Methods Eng* 2002;9:87–140.
- [9] Khandan R, Noroozi S, Sewell P, Vinney J. The development of laminated composite plate theories: a review. *J Mater Sci* 2012;47(16):5901–10. ISSN 0022-2461.
- [10] Lo KH, Christensen RM, Wu EM. A high order theory for plate deformations, part i homogeneous plates. *J Appl Mech* 1977;44:663–8.
- [11] Lo KH, Christensen RM, Wu EM. A high order theory for plate deformations, Part II: laminated plates. *J Appl Mech* 1977;44:669–76.
- [12] Reddy JN, Kim J. A nonlinear modified couple stress-based third-order theory of functionally graded plates. *Compos Struct* 2012;94(3):1128–43. ISSN 0263-8223.
- [13] Carrera E. Historical review of zig-zag theories for multilayered plates and shells. *Appl Mech Rev* 2003;56:287–308.
- [14] Carrera E, Miglioretti F, Petrolo M. Accuracy of refined finite elements for laminated plate analysis. *Compos Struct* 2011;93(5):1311–27.
- [15] Zienkiewicz OC, Taylor RL. *The finite element method*. In: *The Basis*. Butterworth Heinemann; 2000.
- [16] Brezzi F. A discourse on the stability conditions for mixed finite element formulations. *Comput Methods Appl Mech Eng* 1990;82:27–57.
- [17] Boffi D, Brezzi F, Fortin M. *Mixed Finite Element Methods and Applications*. Springer; 2013.
- [18] Bisegna P, Sacco E. A rational deduction of plate theories from the three-dimensional linear elasticity. *ZAMM - J Appl Math Mech/ Zeitschrift für Angewandte Mathematik und Mechanik* 1997;77(5):349–66. ISSN 1521-4001.
- [19] Auricchio F, Sacco E. Partial-mixed formulation and refined models for the analysis of composite laminates within an FSDT. *Compos Struct* 1999;46(2):103–13. ISSN 0263-8223.
- [20] Reissner E. On a certain mixed variational theorem and a proposed application. *Int J Numer Methods Eng* 1984;20:1366–8.
- [21] Reissner E. On a mixed variational theorem and on shear deformable plate theory. *Int J Numer Methods Eng* 1986;23(2):193–8. ISSN 1097-0207.
- [22] Reissner E. On a certain mixed variational theorem and on laminated elastic shell theory. In: *Refined dynamical theories of beams, plates and shells and their applications*. Proceedings of the 29th Euromech Colloquium; 1987. p. 17–27.
- [23] Carrera E. Developments, ideas and evaluations based upon Reissner's mixed variational theorem in the modelling of multilayered plates and shells. *Appl Mech Rev* 2001;54:301–29.

- [24] Chinosi C, Cinefra M, Della Croce L, Carrera E. Reissner's mixed variational theorem toward MITC finite elements for multilayered plates. *Compos Struct* 2013;99:443–52.
- [25] Carrera E. An assessment of mixed and classical theories on global and local response of multilayered orthotropic plates. *Compos Struct* 2000;50(2):183–98. ISSN 0263-8223.
- [26] Carrera E, Demasi L. Classical and advanced multilayered plate elements based upon PVD and RMVT. Part I: derivation of finite element matrices. *Int J Numer Methods Eng* 2002;55:191–231.
- [27] Demasi L. Mixed plate theories based on the generalized unified formulation. Part I: governing equations. *Compos Struct* 2009;87(1):1–11. ISSN 0263-8223.
- [28] Demasi L. Mixed plate theories based on the generalized unified formulation. Part II: layerwise theories. *Compos Struct* 2009;87(1):12–22. ISSN 0263-8223.
- [29] Demasi L. Mixed plate theories based on the generalized unified formulation. Part III: advanced mixed high order shear deformation theories. *Compos Struct* 2009;87(3):183–94. ISSN 0263-8223.
- [30] Demasi L. Mixed plate theories based on the generalized unified formulation. Part IV: zig-zag theories. *Compos Struct* 2009;87(3):195–205. ISSN 0263-8223.
- [31] Demasi L. Mixed plate theories based on the generalized unified formulation. Part V: results. *Compos Struct* 2009;88(1):1–16. ISSN 0263-8223.
- [32] Wu CP, Li HY. The RMVT- and PVD-based finite layer methods for the three-dimensional analysis of multilayered composite and FGM plates. *Compos Struct* 2010;92(10):2476–96. ISSN 0263-8223.
- [33] Wu CP, Li HY. An RMVT-based third-order shear deformation theory of multilayered functionally graded material plates. *Compos Struct* 2010;92(10):2591–605. ISSN 0263-8223.
- [34] Balduzzi G. Beam models: variational derivation, analytical and numerical solutions [Ph.D. thesis]. Univeristá degli Studi di Pavia; 2013.
- [35] Alessandrini SM, Arnold DN, Falk RS, Madureira AL. Derivation and justification of plate models by variational methods. *CRM Proc Lecture Notes* 1999;21:1–20.
- [36] Liu KM. Dimensional reduction for the plate in elasticity on an unbounded domain. *Math Comput Modell* 1999;30(5-6):1–22. ISSN 0895-7177.
- [37] Kantorovich LV, Krylov VI. *Approximate Methods of Higher Analysis*. 3rd ed. P. Noordhoff LTD; 1958.
- [38] Vogelius M, Babuska I. On a dimensional reduction method I. the optimal selection of basis functions. *Math Comput* 1981;37(155):31–46. ISSN 00255718.
- [39] Pagano NJ. Exact solutions for rectangular bidirectional composites and sandwich plates. *Solid Mechanics and Its Applications*, vol. 34. Netherlands: Springer; 1970, ISBN 978-90-481-4451-8. book Section 8, pages 86–101.
- [40] Auricchio F, Sacco E. A mixed-enhanced finite-element for the analysis of laminated composite plates. *Int J Numer Methods Eng* 1999;44(10):1481–504. ISSN 1097-0207.
- [41] Daghia F, de Miranda S, Ubertini F, Viola E. A hybrid stress approach for laminated composite plates within the first-order shear deformation theory. *Int J Solids Struct* 2008;45(6):1766–87. ISSN 0020-7683.
- [42] Moleiro F, Mota Soares CM, Mota Soares CA, Reddy JN. A layerwise mixed least-squares finite element model for static analysis of multilayered composite plates. *Comput Struct* 2011;89(19-20):1730–42. ISSN 0045-7949.
- [43] Auricchio F, Balduzzi G, Lovadina C. A new modeling approach for planar beams: finite-element solutions based on mixed variational derivations. *J Mech Mater Struct* 2010;5(5):27. ISSN 15593959.
- [44] Auricchio F, Balduzzi G, Lovadina C. The dimensional reduction modelling approach for 3d beams: differential equations and finite-element solutions based on Hellinger–Reissner principle. *Int J Solids Struct* 2013;50(25-26):4184–96. ISSN 0020-7683.
- [45] Reddy JN. *Mechanics of Laminated Composite Plates and Shells: Theory and Analysis*. CRC Press; 2004. ISBN 9780849315923.
- [46] Auricchio F, Balduzzi G, Lovadina C. The dimensional reduction modelling approach for 3D beams: Differential equations and finite-element solutions based on Hellinger–Reissner principle. *Int J Solids Struct* 2013;50:4184–96.